Surfactant Behavior of "Ellipsoidal" Dicarbollide Anions: A Molecular Dynamics Study

G. Chevrot, R. Schurhammer, and G. Wipff*

Laboratoire MSM, UMR CNRS 7177, Institut de Chimie, 4 rue B. Pascal, 67 000 Strasbourg, France

Received: February 13, 2006; In Final Form: March 24, 2006

We report a molecular dynamics study of cobalt bis(dicarbollide) anions $[(B_9C_2H_8X_3)_2Co]^-$ (XCD^-) commonly used in liquid−liquid extraction (X = H, Me, Cl, or Br), showing that these anions, although lacking the amphiphilic topology, behave as anionic surfactants. In pure water, they display "hydrophobic attractions", leading to the formation of aggregates of different sizes and shapes depending on the counterions. When simulated at a water/"oil" interface, the different anions (HCD^-, $MeCD^-$, CCD^-, and $BrCD^-$) are found to be surface active. As a result, the simulated M^{n+} counterions (M^{n+} = Na^+, K^+, Cs^+, H_3O^+, UO_2^{2+}, Eu^{3+}) concentrate on the aqueous side of the interface, forming a "double layer" whose characteristics are modulated by the hydrophobic character of the anion and by M^{n+}. The highly hydrophilic Eu^{3+} or UO_2^{2+} cations that are generally "repelled" by aqueous interfaces are attracted by dicarbollides near the interface, which is crucial as far as the mechanism of assisted cation extraction to the oil phase is concerned. These cations interact with interfacial XCD^- in their fully hydrated $Eu(H_2O)_9^{3+}$ and $UO_2(H_2O)_5^{2+}$ forms, whereas the less hydrophilic monocharged cations display intimate contacts via their X substituents. The results obtained with the TIP3P and OPLS models for the solvents are confirmed with other water models (TIP5P or a polarizable 4P−Pol water) and with more polar "oil" models. The importance of interfacial phenomena is further demonstrated by simulations with a high oil−water ratio, leading to the formation of a micelle covered with CCD's. We suggest that the interfacial activity of dicarbollides and related hydrophobic anions is an important feature of synergism in liquid−liquid extraction of hard cations (e.g., for nuclear waste partitioning).

Introduction

Since its first synthesis in 1965,[1] the cobalt bis(dicarbollide) anion $[(B_9C_2H_{11})_2Co]^-$ and its derivatives (Figure 1) found important applications in various domains such as in the medical field as tumor imaging agents,[2,3] in organic synthesis as superacid,[4] and in the partitioning of radioactive ions by liquid−liquid extraction.[5−9] In this context, these hydrophobic anions have first been used in combination with complexing agents such as PEG and CMPO molecules for the simultaneous extraction of Cs^+, Sr^{2+}, and actinides (Russian UNiversal EXtraction "UNEX" process[10,11]). When added as synergistic agents to extractant molecules such as crown ethers, calixarenes, phosphoryl derivatives,[12−16] or grafted onto such chelating platforms,[17,18] they markedly improve the ion extraction efficiency. So far, little is known, however, on the solution properties of these anions in pure liquids or heterogeneous liquid mixtures and on the mechanism of synergistic extraction.[19,20]

This led us to undertake molecular dynamics simulations on solutions containing dicarbollide anions of general $[(B_9C_2H_8X_3)_2Co]^-$ formula, where X = H, Me, Cl, and Br. They will be noted generically as XCD^- and specifically as HCD^-, $MeCD^-$, CCD^-,[21] and $BrCD^-$, respectively. We first study the effect of the X substituents on the solvation of XCD^- and the nature of the XCD^-, H_3O^+ and CCD^-, Cs^+ ion pairs, comparing concentrated pure water and pure "oil" (chloroform) solutions. We then focus on the interfacial behavior of different salts at a chloroform/water interface. In the XCD^- Cs^+ series, we want to assess the effect of the X substituents on the interfacial behavior of the ions. We then study the effect of M^{n+} counterions on the distribution and solvation of a given anion, choosing the commonly used chlorinated CCD^- derivative and Na^+, K^+, Cs^+, H_3O^+, UO_2^{2+}, and Eu^{3+} as counterions. This will allow us to investigate the effect of cation size and hydrophilicity in the alkali cation series, and the effect of cation charge in the alkali, uranyl, and europium series. The anions are often used in their acidic form, and the comparison of H_3O^+ versus K^+ or Cs^+ will give insights into the nature of ion pairs and of possible hydrogen bonding interactions between H_3O^+ and CCD^-. These simulations will be based on water−oil mixtures in similar proportions (about 50:50 in volume). As in extraction experiments where the receiving phase becomes gradually oil-rich, we will also consider a concentrated solution of CCD^-, Cs^+ in a 90:10 oil−water mixture, with the aim to elucidate the basis of synergistic effects of dicarbollide ions in liquid−liquid extraction.

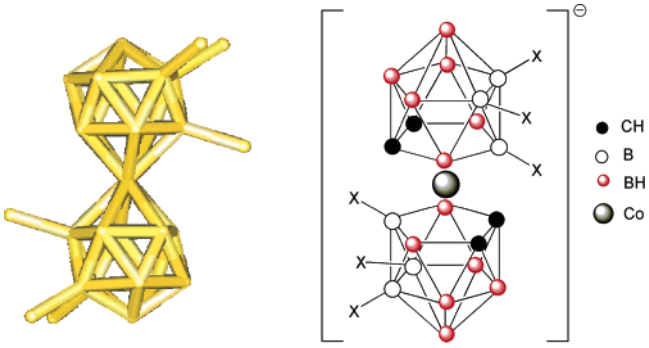

Figure 1. Dicarbollide XCD^- anions (hydrogens not shown for clarity).

* Corresponding author. E-mail: wipff@chimie.u-strasbg.fr.

10.1021/jp060930q CCC: $33.50
Published on Web 04/22/2006

TABLE 1: Selected Atomic Charges of XCD^- Obtained from Different Methods[a]

	X = H[b]			X = Me[b]			X = Cl				X = Br[b]		
	Mulliken	ESP	NPA	Mulliken	ESP	NPA	ESP[c]	Mulliken[b]	ESP[b]	NPA[b]	Mulliken	ESP	NPA
Co	−0.43	0.09	1.29	−0.93	−0.26	1.29	0.18	−0.29	−0.38	1.29	−0.18	0.26	1.27
X[d]	−0.04	−0.11	0.06	−0.21	−0.25	−0.22	−0.29	−0.17	−0.18	−0.15	−0.30	−0.11	−0.06
CH[e]	−0.11	0.13	−0.29	−0.12	0.09	−0.29	0.04	−0.10	0.21	−0.28	−0.11	0.18	−0.28

[a] A full version is given in Table S1. [b] DFT/6-31G* calculation. [c] HF/3-21G* calculation. [d] Averages over the six X substituents. [e] Averages over the four CH's.

Methods

Molecular Dynamics. Molecular dynamics simulations were performed with the AMBER 7.0[22] software and the AMBER force field[23] with the following representation of the potential energy U:

$$U = \sum_{\text{liaisons}} k_l(l - l_0)^2 + \sum_{\text{angles}} k_\theta(\theta - \theta_0)^2 + \sum_{\text{dièdres}} \sum_n V_n(1 + \cos(n\varphi - \gamma)) + \sum_{i<j} \left[\frac{q_i q_j}{R_{ij}} - 2\epsilon_{ij}\left(\frac{R_{ij}^*}{R_{ij}}\right)^6 = \epsilon_{ij}\left(\frac{R_{ij}^*}{R_{ij}}\right)^{12} \right]$$

It accounts for the deformation of bonds, angles, dihedral angles, electrostatic, and van der Waals interactions. For the dicarbollide anions, the l_0 and θ_0 values were taken from experiment.[24] Note that previous MD simulations on CCD^- assumed that all internal angles were 109° for simplicity.[19,20] Because of the constrained topology of CCD^-, this was of little consequence for its geometry, which was well reproduced by this force field, but the diffusion of CCD^- was quite slow during the dynamics, too much heat being associated with internal motions. This drawback disappeared with the updated parameters. The CH and BH groups of CCD^-, HCD^-, $BrCD^-$, and $MeCD^-$ were represented with the united atom representation, and these anions were fixed with a trans arrangement of the two $C_2B_9H_8X_3$ caps, consistent with QM results.[19,25]

The Lennard−Jones parameters for the Na^+, K^+, Cs^+,[26] UO_2^{2+},[27] and Eu^{3+} [28] cations were fitted on their free energies of hydration. The solvents were represented explicitly at the molecular level, using the TIP3P model[29] for water and the OPLS model for chloroform.[30] Tests with other models, namely the TIP5P[31,32] and polarizable "4P−Pol"[33] models for water, and scaled models of chloroform (vide infra) were also performed. Nonbonded interactions were calculated with a 12 Å atom-based cutoff, correcting for the long-range electrostatics by using the Ewald summation method (PME approximation). The solutions were simulated with 3D-periodic boundary conditions, thus as alternating slabs of water and "oil", forming two interfaces.

For the XCD^- anions, two sets of ESP charges have been used, both fitted on electrostatic potentials. The 3-21G* charges of CCD^- (X = Cl) come from refs 19 and 20 and have been derived from HF/3-21G* calculations on a structure adapted from the X-ray structure of $BrCD^-$.[24] They have been used for the systems containing CCD^- with different M^{n+} counterions. The 6-31G* charges were derived to study the XCD^- series (X = H/Cl/Br/Me), based on DFT-B3LYP/ 6-31G* optimized structures, using the Gaussian 03 software.[34] The ESP charges and the corresponding Mulliken and natural population analysis (NPA) charges are given in Tables 1 and S1 (Supporting Information). As expected, there is a broad disparity in charges as a function of their definition, particularly for the Mulliken charges, which are known to be basis set dependent. This is less the case with the NPA charges with which, e.g., the q_{Co} charge on cobalt is fairly constant (+1.3 e) in all studied anions. Interactions with the medium depend on the distribution of electrostatic potential ϕ around the surface, and ϕ is found to be rather insensitive to the choice of charges (see the case of CCD^- in Figure S1, Supporting Information). Furthermore, its distribution around the different XCD^- anions is similar, i.e., negative and highly delocalized over the whole anion (Figure S1, Supporting Information). In the case of HCD^- and $MeCD^-$ anions, ϕ is somewhat more negative near the equatorial region, i.e., between the two borocarbon caps.

The interface was built from adjacent boxes of water and chloroform.[35] Unless otherwise specified, all solutions contain 30 XCD^- anions neutralized by 30 M^+, 15 UO_2^{2+}, or 10 Eu^{3+} cations, corresponding to an aqueous concentration of ≈0.4 mol/L. The XCD^- M^{n+} ions were initially immersed "at the interface" ($z = 0$), half in water and the other half in chloroform (Figure 2). After 1000 steps of energy minimization (100 steps by the steepest descent + 900 steps by conjugate gradients), we performed 50 ps of MD with fixed solutes ("BELLY" option of AMBER) and 50 ps without constraints, followed by 50 ps at a constant pressure of 1 atm (monitored with a weak coupling method[36]). The production stage was performed at 300 K in the (N, V, T) ensemble for at least 2 ns. The temperature was maintained constant by coupling the solution to a thermal bath using the Berendsen algorithm[36] with a relaxation time of 0.2 ps. The main characteristics of the systems are summarized in Table 1.

The coordinates were saved every 0.5 ps and analyzed using the MDS and DRAW software.[37] Snapshots were redrawn with the VMD software.[38] The position of the interface was dynamically defined as the intersection between the water and oil density curves.[39] The percentage of ions "at the interface" was calculated during the last 0.75 ns, selecting the species that are within 10 Å from the interface. We defined the density of solvents and solutes ($g \cdot cm^{-3}$) at a z-position by their mass per volume unit ($dv = xy\,dz$). Insights into energy components were obtained from the average interactions between selected groups during the last 0.4 ns, calculated with a 17 Å cutoff distance and a shift cutoff correction. The ion−ion and ion−solvent environments were characterized by the radial distribution functions (RDFs) during the last 0.25 ns. The average coordination numbers (noted CN) were obtained by integration of the first peak of the RDFs. The self-diffusion coefficient D was calculated during the last nanosecond with the Einstein relation:

$$D = \frac{1}{6}\lim_{t\to\infty}\frac{d}{dt}\langle|r_i(t) - r_i(0)|^2\rangle$$

where $r_i(t)$ is the position of atom i at the time t.

Free Energy Calculations. The changes in free energies of solvation ΔG between XCD^- and YCD^- anions were obtained

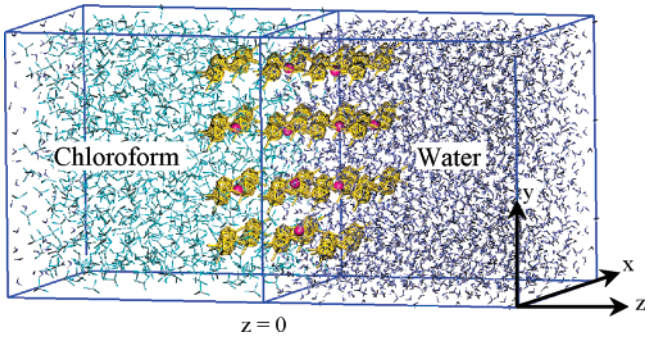

Figure 2. The chloroform/water interface with 30 CCD^- and 10 Eu^{3+}. Initial position (0 ns) with the solute "perpendicular" to the interface.

by free energy perturbation FEP calculations[40] using the windowing technique based on the following equation:

$$\Delta G_{\lambda_i} = G_{\lambda_{i+1}} - G_{\lambda_i} = -RT \ln\left\langle \exp - \frac{U_{\lambda_{i+1}} - U_{\lambda_i}}{RT} \right\rangle_{\lambda_i}$$

where R is the molar gas constant and T is the absolute temperature. $\langle\ \rangle$ stands for the ensemble average at the state λ_i where U_{λ_i} is the potential energy. The mutation of XCD^- ($\lambda = 0$) to YCD^- ($\lambda = 1$) was achieved via hybrid van der Waals parameters of the substituents X and Y ($R^*_\lambda = \lambda R^*_1 + (1 - \lambda) R^*_0$; $\epsilon_\lambda = \lambda\epsilon_1 + (1 - \lambda)\epsilon_0$) and hybrid charges ($q_\lambda = \lambda q_1 + (1 - \lambda) q_0$). For $MeCD^-$, the methyl groups were represented with the united atom representation.[41] The mutations were achieved in 50 windows, i.e., with increments $\Delta\lambda$ of 0.02. At each window, 4 ps of equilibration were followed by 6 ps of MD for data collection, calculating the difference in free energies between the states λ and $\lambda + \Delta\lambda$ ("forward calculation") and between the states λ and $\lambda - \Delta\lambda$ ("backward calculation"). In each case, the changes of free energy ΔG were averaged from independent simulations from one anion to another and vice versa.

Results

I. Dicarbollides in Pure Water and in Pure Chloroform Solutions. In this section, we first describe the solvation of a single XCD^- anion (without counterion) in water and in chloroform to compare the solvation energies as a function of the X substituents (Tables 3 and 4). This is followed by the study of concentrated systems (30 XCD^-, H_3O^+, and 30 CCD^-, Cs^+), looking at the nature of supramolecular organization in these two solvents.

1. Effect of X Substituents: The XCD^- Anion in Diluted Aqueous and Chloroform Solutions. We first analyze the average interaction energies E_{solv} between a given XCD^- anion and water or chloroform. The results (Table 3) show that E_{solv} is negative and more attractive with water (−75 to −88 kcal/mol) than with chloroform (−42 to −50 kcal/mol). The interactions are mainly of electrostatic origin in water and involve similar contributions of van der Waals and electrostatic components in chloroform. In water, the E_{solv} energies decrease in magnitude in the order: $HCD^- < MeCD^- < BrCD^- \approx CCD^-$, indicating that the smallest anion best interacts with water. This differs from the chloroform solution with which the $MeCD^-$ anion displays the strongest interaction, while the three other anions have very close E_{solv} energies. Note that, for the CCD^- anion, the E_{solv} energies obtained with the 6-31G* and 3-21G* charges are similar (within 3 and 1 kcal/mol, respectively) and small, compared to the effect of the X substituent.

TABLE 2: Characteristics of the Simulated Systems with 30 XCD^- 30/n M^{n+} Salts[a]

	N_{oil}/N_{water}	time (ns)	box size (Å^3)
XCD^- M^+ in pure chloroform			
CCD^- Cs^+ [b]	1330/0	3	60 × 60 × 60
CCD^- H_3O^+ [b]	1450/0	1	60 × 60 × 60
CCD^- H_3O^+ [c]	1443/0	1	60 × 60 × 60
HCD^- H_3O^+ [c]	1467/0	1	60 × 60 × 60
$MeCD^-$ H_3O^+ [c]	1408/0	1	60 × 60 × 60
$BrCD^-$ H_3O^+ [c]	1437/0	1	60 × 60 × 60
XCD^- M^+ in pure water			
CCD^- Cs^+ [b]	0/6693	2	61 × 61 × 61
CCD^- H_3O^+	0/6459	2	60 × 60 × 60
Chloroform/Water Interface			
XCD^- Cs^+ salts[c]			
HCD^- Cs^+	869/3879	2.5	50 × 50 × 100
$MeCD^-$ Cs^+	830/3824	2.5	50 × 50 × 100
CCD^- Cs^+	840/3856	2.4	51 × 51 × 101
$BrCD^-$ Cs^+	855/3862	2.6	51 × 51 × 101
CCD^- M^{n+} salts[b]			
CCD^- Cs^+	855/3931	2.5	50 × 50 × 100
CCD^- UO_2^{2+}	860/3955	2.3	50 × 50 × 100
CCD^- Eu^{3+}	850/3905	2.5	50 × 50 × 100
CCD^- Eu^{3+} [d]	757/4178	2.5	50 × 50 × 100
CCD^- Na^+	867/3931	2.4	51 × 51 × 102
CCD^- K^+	861/3959	2.5	51 × 51 × 102
CCD^- H_3O^+	844/3871	2.5	50 × 50 × 100
CCD^- Cs^+ [b] in 90:10 oil/water mixture. Cubic box			
CCD^- Cs^+	1158/524	3.0	59 × 59 × 59
Interfaces with TIP5P water and OPLS chloroform			
30 CCD^- 30 Cs^+ [b]	865/3931	2.6	51 × 51 × 101
30 CCD^- 10 Eu^{3+} [b]	851/3920	2.76	50 × 50 × 101
Interfaces with 4P−Pol water and OPLS chloroform			
30 CCD^- 10 Eu^{3+} [b]	851/3868	2.5	51 × 51 × 102
Interfaces with modified chloroform and TIP3P water			
CHLOR-1: CCD^- Cs^+ [b]	865/3931	2.5	50 × 50 × 100
CHLOR-2: CCD^- Cs^+ [b]	865/3918	2.5	50 × 50 × 100
CHLOR-3: CCD^- Cs^+ [b]	865/3918	2.5	50 × 50 × 100

[a] Number of solvent molecules, simulated time and box size. [b] The CCD^- anions are modeled with 3-21G* ESP charges. [c] The XCD^- anions are modeled with 6-31G* ESP charges. [d] The simulation start with the CCD^- ions in chloroform and Eu^{3+} in water (see Figure 9).

Further insights into the relative free energies of solvation ΔG_{solv} as a function of the X substituent were obtained by free energy calculations, whose results are reported Table 4. From independent simulations performed both ways, it can be seen that the hysteresis is small (<1 kcal·mol^{-1}) and that, in water, ΔG_{solv} follows the order: $HCD^- > MeCD^- > CCD^- \approx BrCD^-$, confirming that the smallest anion is best hydrated, and that the CCD^- and $BrCD^-$ anions with Cl versus Br halogens are similarly hydrated ($\Delta\Delta G = 0.5$ kcal·mol^{-1}) and are the most hydrophobic. In chloroform, the order differs from that in water, as $MeCD^-$ is best solvated: $MeCD^- > CCD^- > HCD^- > BrCD^-$, which does not simply follow the size of the XCD^-. Furthermore, comparing CCD^- with two sets of charges (via the mutation of 6-31G* to 3-21G* charges) shows that the ΔGs are close to zero in water (0.6 kcal/mol) and in chloroform (−0.04 kcal/mol), indicating that CCD^- is equally well solvated with these two sets of charges, allowing us to directly compare the results obtained with one set or the other, also supported by the results in solution (vide infra).

The hydration structure of XCD^- anions (see snapshots and RDFs in Figure S2, Supporting Information) is similar with the different X substituents. No water directly coordinates to the cobalt atom, which is shielded by the borocarbon caps. The H_{H_2O}

TABLE 3: Average Interactions Energies E_{Solv} and Fluctuations (in kcal·mol^{-1}) of an XCD$^-$ Anion with Pure Water and Pure Chloroform[a]

	HCD$^-$		MeCD$^-$		CCD$^-$		BrCD$^-$		CCD$^-$ [b]	
water	-88 ± 7		-84 ± 7		-75 ± 6		-77 ± 6		-72 ± 6	
	-81 ± 7	-7 ± 2	-71 ± 7	-13 ± 2	-60 ± 6	-15 ± 2	-62 ± 6	-15 ± 2	-57 ± 6	-15 ± 2
chloroform	-42 ± 5		-50 ± 6		-43 ± 4		-42 ± 4		-42 ± 4	
	-28 ± 4	-15 ± 4	-22 ± 4	-28 ± 2	-17 ± 4	-25 ± 2	-17 ± 4	-25 ± 2	-17 ± 4	-25 ± 2

[a] Electrostatic and van der Waals components on the 2nd line. Unless other specifications, XCD$^-$ was simulated with 6-31G* charges. [b] The CCD$^-$ anion is modeled with 3-21G* ESP charges.

TABLE 4: Differences in Free Energies of Solvation ΔG_{Solv} (in kcal·mol^{-1}) of XCD$^-$ Anions in Water and in Chloroform[a]

			water	chloroform
HCD$^-$	→	MeCD$^-$	+3.43	−5.05
MeCD$^-$	→	HCD$^-$	−2.78	+4.75
MeCD$^-$	→	CCD$^-$	+4.58	+4.49
CCD$^-$	→	MeCD$^-$	−4.65	−4.34
CCD$^-$	→	BrCD$^-$	+0.54	+2.11
BrCD$^-$	→	CCD$^-$	−0.40	−1.96
CCD$^-$ (6-31G*)	→	CCD$^-$ (3-21G*)	+0.60	−0.04

[a] Unless other specifications, XCD$^-$ was simulated with 6-31G* charges.

protons make shorter contacts than the O_{H_2O} atoms with the anions, which is typical for anionic solvation. The resulting hydrogen bonds are rather weak and nonspecific, as confirmed by AMBER and quantum mechanical calculations on the XCD$^-$···H_2O dimers.[42]

Chloroform does not display specific interactions with the HCD$^-$, MeCD$^-$, CCD$^-$, and BrCD$^-$ anions, as seen from the RDFs of Cl and C atoms of $CHCl_3$ around the Co or X atoms of the anion (Figure S2, Supporting Information).

2. Aggregation of XCD$^-$ M$^+$ Salts (M$^+$ = H$_3$O$^+$/Cs$^+$) in Chloroform and Water Solutions. Dicarbollides are weakly soluble in halogenated organic solvents. For instance, the solubilities of NaHCD and CsHCD in 1,2-dichloroethane are ca. 10^{-2} M and 1.8×10^{-4} M, respectively.[43] To our knowledge, no data have been reported in water (see, however, ref 44) but the salts should be less soluble than they are in organic solvents, as they generally partition to the organic phase in extraction experiments. It is thus interesting to investigate the nature of concentrated solutions, to determine to which extent the salts will dissolve in such solvents. In this section, we consider oversaturated solutions (with 30 ion pairs per box, which corresponds to ca. 0.23 M concentrations), comparing the "oil" to the aqueous solutions, and H_3O^+ versus Cs^+ as counterions. For computer time-saving purposes, the effect of X substituent on the anion will be studied with the XCD$^-$ H_3O^+ salts in chloroform and, in water, only the CCD$^-$ H_3O^+ and CCD$^-$ Cs^+ will be considered.

Chloroform is not polar enough to stabilize solvent-separated or -dissociated ion pairs, and as a result, the ions of the different salts collapsed to form a single droplet (Figure 3).[45] This "microphase" is overall neutral, reminiscent of molten salts or ionic liquids[46] where each ion tends to be surrounded by counterions, sometimes forming chain-type sequences of the XCD$^-$···H_3O^+···XCD$^-$ type in the XCD$^-$ series, and of the CCD$^-$···Cs^+···CCD$^-$ type with Cs^+. No ion is fully solvated by chloroform. As seen on snapshots and RDFs (Figure S3, Supporting Information), the anions interact with the H_3O^+ protons via their X substituents in the case of HCD$^-$, CCD$^-$, or BrCD$^-$. The only exception concerns MeCD$^-$, which mostly interacts via its BH protons, rather than via its methyl groups,

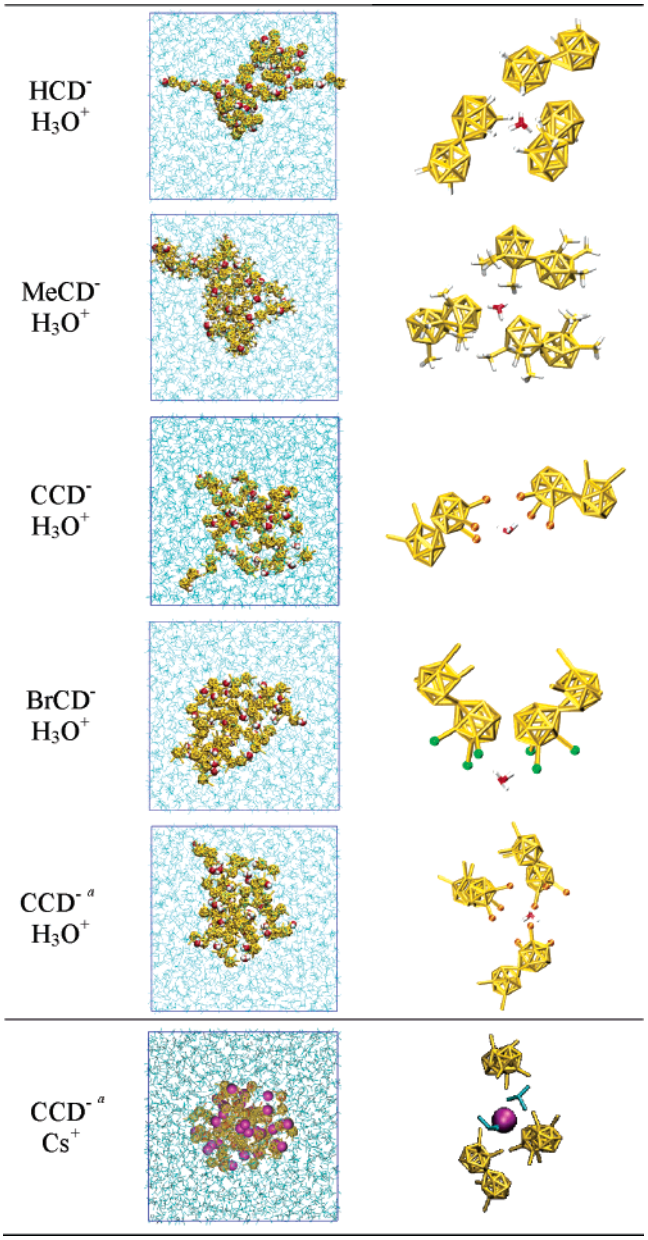

Figure 3. XCD$^-$ H_3O^+ (X = H/Me/Cl/Br) and CCD$^-$ Cs^+ salts in pure chloroform. Final snapshots. Unless other specifications, XCD$^-$ was simulated with 6-31G* charges. A full version with RDFs is given in Figure S3, Supporting Information. [a] CCD$^-$ with 3-21G* charges.

with $H_{H_3O^+}$. In the case of the CCD$^-$ Cs^+ salt, the anions preferentially interact with Cs^+ via their B−Cl substituents, as they do with H_3O^+. Comparing the Cs^+ CCD$^-$ with the H_3O^+ CCD$^-$ aggregates, one sees that the former is more compact because Cs^+ is spherical and therefore less stereochemically demanding than H_3O^+. As a result, Cs^+ coordinates more CCD$^-$ anions than H_3O^+ does (4.7 versus 3.8 anions, on the average per cation).

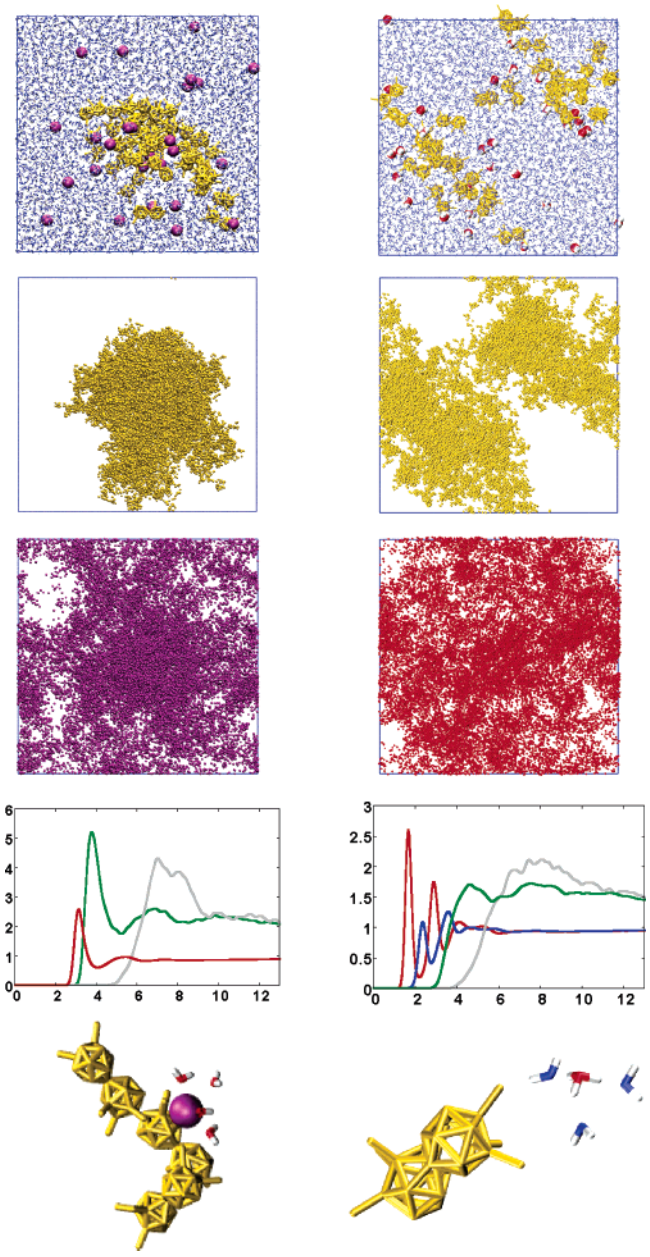

Figure 4. CCD^- Cs^+ (left) and CCD^- H_3O^+ salts (right) in pure water. From top left to bottom right: Final snapshots. Cumulated views of Co (during the last 1 ns). Cumulated views of M^+ (during the last 1 ns). RDFs around Cs^+ and $H_{H_3O^+}$ (O_{wat} (in red), Co (in gray), and Cl_{CCD} (in green), H_{wat} (in blue)). Snapshots of typical Cs^+ and H_3O^+ environments.

Water is a more dissociating solvent than chloroform. However, when the CCD^- H_3O^+ and CCD^- Cs^+ salts are simulated in aqueous solution, they do not dilute because the anions tend to aggregate (see Figure 4). These are hydrophobic and somewhat "attract each other" in water due to solvophobic forces, and there is more anion aggregation with Cs^+ than with H_3O^+ as counterion. The anionic aggregates are dynamic in nature and instantaneously quite asymmetrical and irregular, especially with H_3O^+ counterions. The cumulated trajectories clearly reveal a single anionic domain with Cs^+, and two more "diluted domains" with H_3O^+. According to the Co−Co RDFs, a given anion is surrounded on the average by 6.6 CCD^- in the case of the Cs^+ salt, and by 4.4 CCD^- in the case of the H_3O^+ acid, within 15 Å. This is less than in chloroform solution (≈10 CCD^-) because the aggregate is more diluted in water due to the fact that the majority of H_3O^+ or Cs^+ counterions are well hydrated (by 3.0 and 7.2 H_2O molecules, on the average) and diluted in "bulk water". They have thus no contact at all (in the case of H_3O^+) or limited contacts (1.2 CCD^-, on the average in the case of Cs^+) with CCD^- anions.

II. Dicarbollide Salts at the Chloroform/Water Interface. Unless otherwise specified, all simulations at the interface started with two grids of ions "perpendicular to the interface", equally shared between the two solvents (Figure 2) and, in all cases, the ions that were in the organic phase diffused to the interface or to bulk water. The simulations show that the dicarbollide anions concentrate on the aqueous side of the interface without forming, however, regular monolayers. Their distribution is modulated by the hydrophobic character of the anion in the XCD^- series and by the nature of the metallic counterions for a given anion.

1. The Effect of X Substituent in the 30 XCD^-, Cs^+ Series. The different simulated XCD^- anions adsorb at the interface and attract the majority of Cs^+ counterions (see Figure 5).[45] The proportion of anions at the interface(s) is found to depend on the X substituent and ranges from 67% for HCD^- to 98% for $BrCD^-$, thus increasing with the hydrophobic character of the anion. As a result, there is a high proportion of Cs^+ counterions at the interface, which also increases, from 53% in the case of the HCD^- salt to 70% in the case the $BrCD^-$ salt. Another consequence is that the more hydrophobic $BrCD^-$ and CCD^- anions all remained at the same interface during the dynamics, whereas some HCD^- and $MeCD^-$ anions migrated from one interface to the other via the water phase during the dynamics. As a result, these anions are more diluted than their more hydrophobic analogues at a given interface.

The Cs^+ cations sit deeper in water than the anions, and as shown by the analysis of the RDFs and typical snapshots (Figures 5 and S4, Supporting Information), they are mostly surrounded by water.[45] At the interface, Cs^+ and the anions sometimes form loose contact pairs, involving up to 3−4 anions per Cs^+, thereby reducing its hydration. One thus finds less water around Cs^+ at the interface (5.6 H_2O, on the average in the case of the CCD^- Cs^+ salt) than in pure water (9 H_2O). Comparing the average hydration number of all Cs^+ ions yields 8.1, 8.1, 5.9, and 5.2 H_2O on the average, respectively with HCD^-, $MeCD^-$, CCD^-, and $BrCD^-$ anions. The Cs^+ hydration thus decreases as a result on enhanced pairing with XCD^- anions when the latter are more hydrophobic and more surface active.

2. The Effect of M^{n+} Counterions with CCD^- Anions. In this section, we consider a same type of anion (CCD^-), and compare M^{n+} counterions of different charges ($Na^+/UO_2^{2+}/Eu^{3+}$) or of different sizes ($Na^+/K^+/Cs^+$). During the dynamics, most ions concentrated near the interface, while the remaining ones diluted in water (Figure 6). Interesting trends are observed, depending on M^{n+}, as discussed below.

Charge Effect of M^{n+} Counterions ($Na^+/UO_2^{2+}/Eu^{3+}$). For the UO_2^{2+} and Eu^{3+} containing solutions, the percentages of CCD^- anions at the interface (68% for both systems) and of cations (79% and 74%, respectively) are quite high and comparable. As seen from density curves, the cations are more remote than the anions from the interface: their respective densities peak at 9.6 and 4.7 Å for UO_2^{2+} CCD^-, and 11.2 and 6.0 Å for Eu^{3+} CCD^-, respectively. In the case of the CCD^- Na^+ solution, however, there are less anions (60%) and cations (47%) at the interface and therefore more in "bulk water" than with the harder cations, showing that the interfacial activity of the cation depends not only on its hydrophilic/hydrophobic

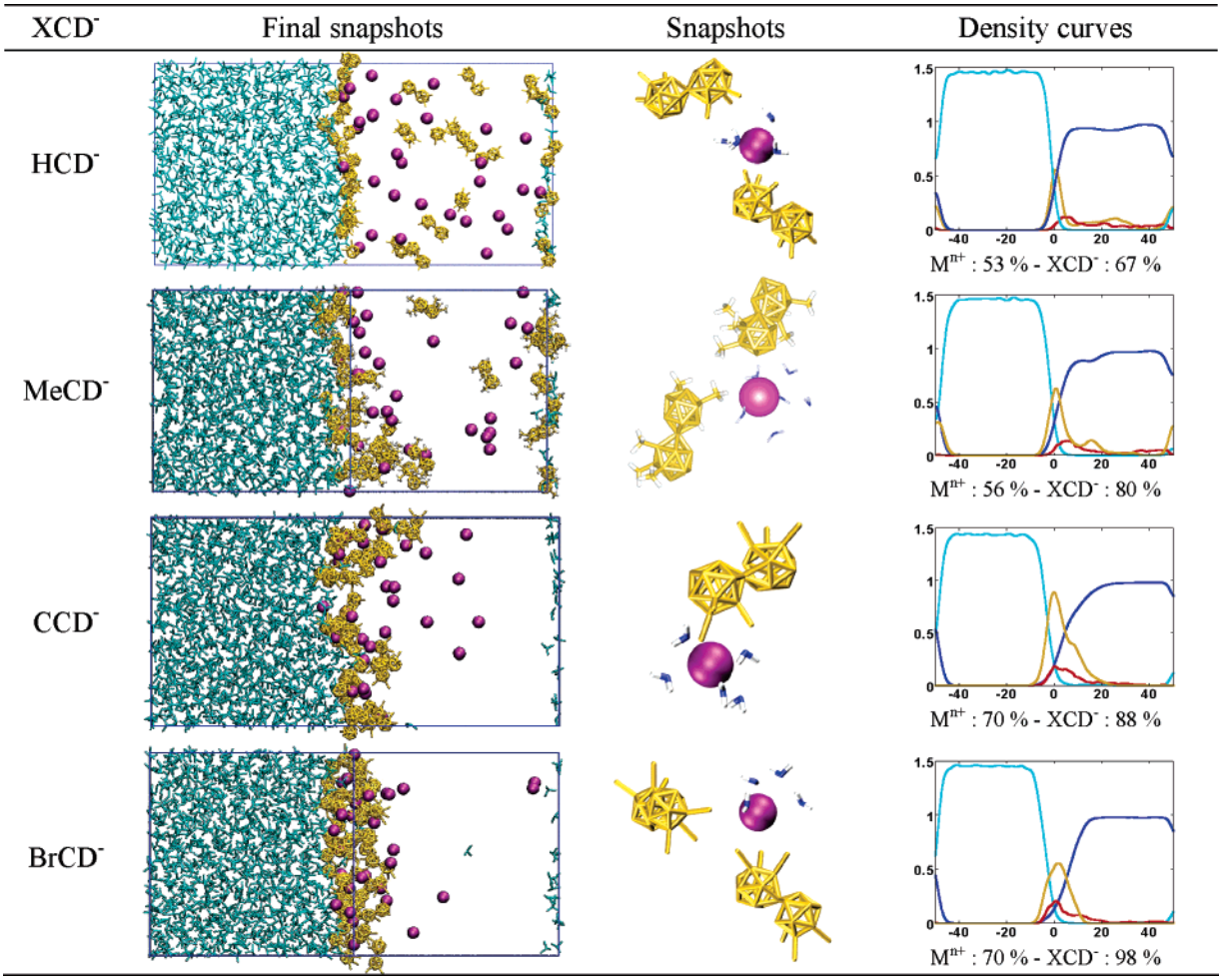

Figure 5. XCD^- Cs^+ salts at the interface. Final snapshots (water not shown for clarity), zoom on Cs^+ XCD^- ions, density curves (chloroform in cyan, water in blue, XCD^- in brown, and Cs^+ in red) and percentages of ions within 10 Å from the interface, including the two interfaces in the case of the HCD^- Cs^+ and $MeCD^-$ Cs^+ salts.

balance, but also on its attractions with the anionic layer, which are stronger with Eu^{3+} than with Na^+.

Generally, hard cations are "repelled" by the interface, and the high concentration of Eu^{3+} near the interface may be quite surprising. To assess that this does not artifactually result from the sampling issue, we decided to run another simulation of the Eu^{3+} CCD^- solution, starting with the cations in the water phase (i.e., as far from the interface), and the anions in the oil phase (see Figure 7). In fact, during the dynamics, nearly all (90%) CCDs moved to one interface, thereby attracting the Eu^{3+} cations, whose proportion at the interface (85%) is even larger than in the simulation which started with a symmetrical distribution (74%), showing that the observed interfacial activity of Eu^{3+} ions does not critically depend on the starting configuration. The main difference with the simulation which started with a "symmetrical" ion distribution is that the ions are now diluted onto two interfaces, instead of concentrating at a single one. As a result of lessened anion−anion repulsions at the interface, the proportion of the anions and cations at the interfaces is higher.

In the Na^+, UO_2^{2+}, and Eu^{3+} containing solutions, the cations, be they at the interface or in bulk water, are fully hydrated and thus mainly interact with CCD^- as $Na(H_2O)_6^+$, $UO_2(H_2O)_5^{2+}$, and $Eu(H_2O)_9^{3+}$ species, respectively (see snapshots in Figure 6 and RDFs in Figure S4, Supporting Information). In fact, some cations may be surrounded by a "cage" of up to four CCDs at the interface, forming solvent-separated "ion pairs" of the $M^{n+}\cdots OH_2\cdots CCD^-$ type.

Comparison of Different Monocharged Counterions (Na^+/K^+/Cs^+/H_3O^+). In the series of CCD^- M^+ salts with different M^+ counterions, the majority of anions also adsorb at the interface, thereby attracting the M^+ cations. There is, again, an interesting evolution in the Na^+/K^+/Cs^+ series (Figure 6) as the proportion of CCD^- anions at the interface increases with the lessened hydrophilic character of M^+ (from 60 to 82 and 93%, respectively) as the proportion of M^+ cations does (from 60 to 71%). Thus, the less hydrophilic the cations, the higher the surface activity of CCD^-. All CCD^- ions adsorb at a single interface, except in the case of K^+ CCD^-, where some of them migrated from one interface to the other via the water slab. In the case of the acidic solution with CCD^- H_3O^+ ions, the amount of CCDs at the interface (80%) is similar to the one in the CCD^- K^+ solution.

According to the RDFs (Figure S4, Supporting Information), the Na^+, K^+, and Cs^+ cations are hydrated by 5.8, 6.5, and 5.8 H_2O molecules, respectively, on the average. The bigger the cation, the higher its tendency to pair with CCD^-. As a result, the number of Cl(CCD) atoms coordinated to M^+ increases from 0.0 (Na^+) to 0.2 (K^+) and 2.4 (Cs^+) on the average, which explains why the biggest cation Cs^+ is less hydrated than K^+. Concerning the H_3O^+ ion, it is hydrogen bonded to 3 H_2O molecules as in pure water and mainly interacts

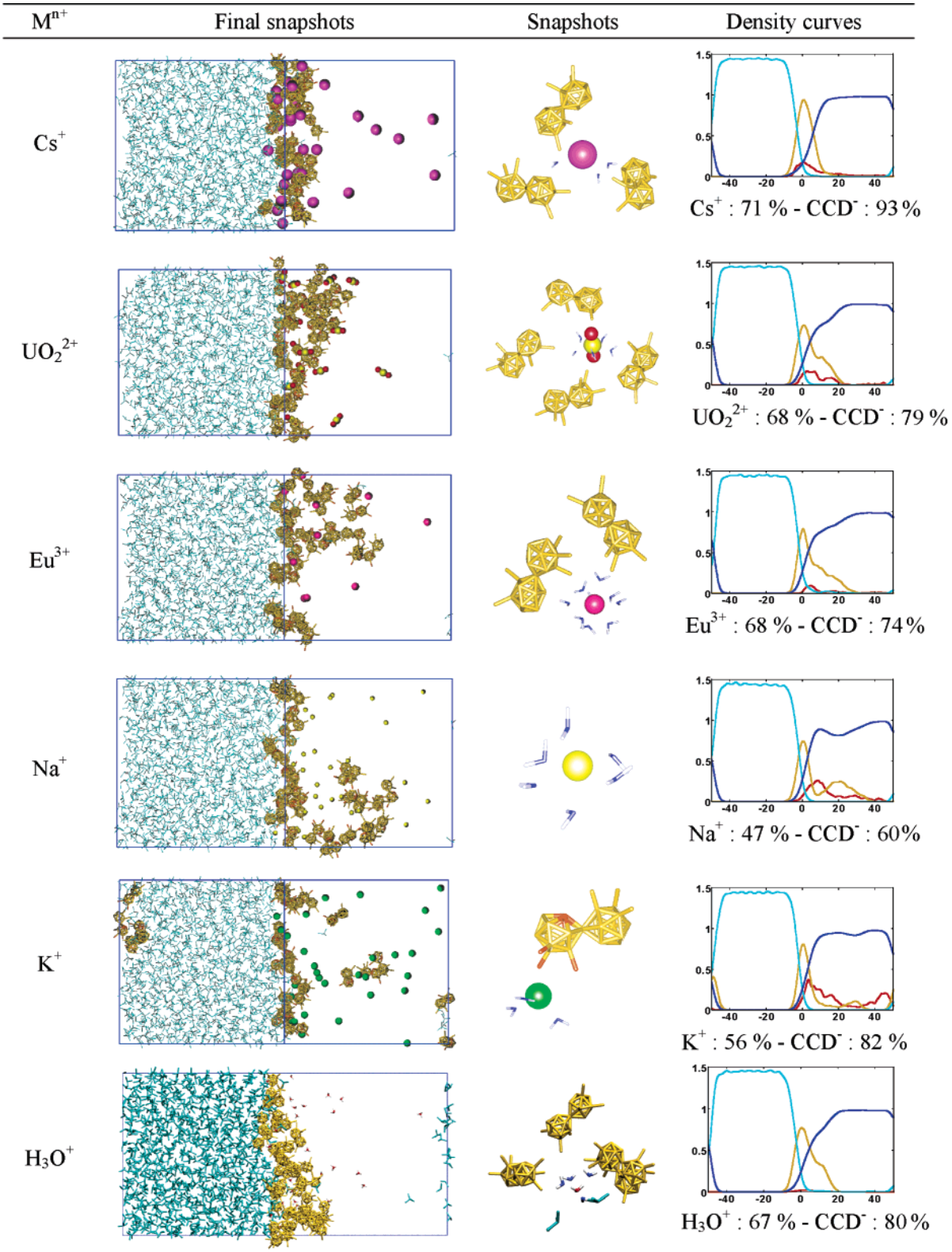

Figure 6. CCD^- M^{n+} salts (with $M^{n+} = Cs^+$, UO_2^{2+}, Eu^{3+}, Na^+, K^+, and H_3O^+) at the interface. Final snapshots (water is not shown for clarity), zoom on M^{n+} XCD^- ions, density curves (chloroform in cyan, water in blue, XCD^- in brown, and M^{n+} in red), and percentages of ions within 10 Å from the interface, including the two interfaces in the case of the CCD^- K^+ salt.

via $H_3O^+\cdots HOH\cdots CCD^-$ interactions, never making direct hydrogen bonds with CCD^-.

3. 30 CCD^-, Cs^+ Ions in Water-in-Oil Emulsions. As in liquid−liquid extraction experiments, where the oil/water ratio progressively increases as one moves from the aqueous to the oil phase, we decided to simulate an oil-rich solution of Cs^+ CCD^- with an oil/water 90:10 volume ratio in a cubic box of solvent, starting as above with a grid of ions "perpendicular to the interface". During the dynamics, the ions and solvents rearranged to form an irregular water-in-oil micelle (Figure 8), whose interface is more or less covered by the CCD^- anions and Cs^+ cations, in equilibrium with CCD^-Cs^+ oligomers.

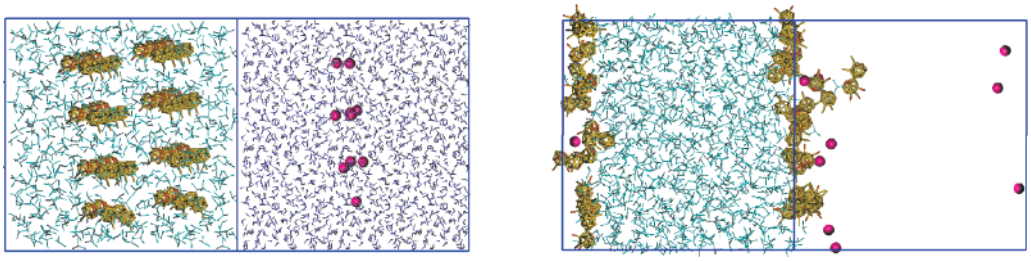

Figure 7. CCD^- Eu^{3+} salts simulated at the interface starting with all CCD^- in chloroform and all Eu^{3+} in water. Initial (left) and final (right) snapshots.

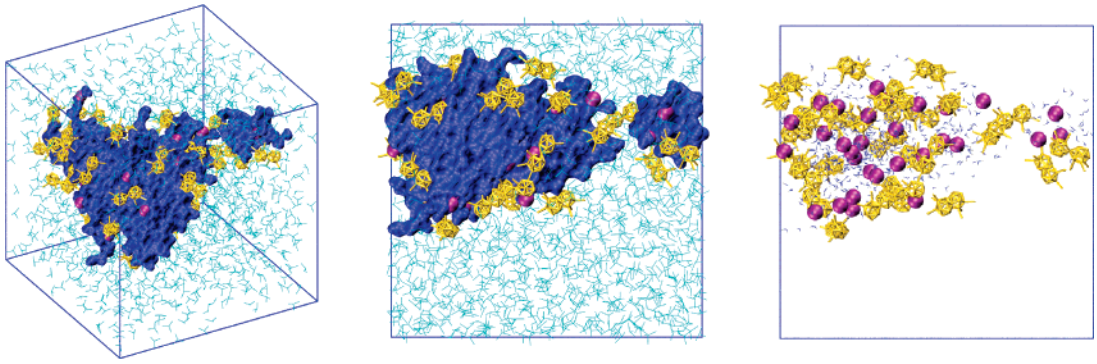

Figure 8. The CCD^- Cs^+ salt simulated in a 90:10 oil/water mixture. Final snapshots showing the ions and, separately, the chloroform molecules and the water surface with two different orientations (left and middle) and the water molecules (right).

Interestingly, the Cs^+ environment is, on the average, quasi the same with the 90:10 as with the 50:50 oil/water ratio (5.8 O(H_2O) and 2.4 Cl(CCD) atoms on the average).

Discussion and Conclusions

We report MD investigations on the solution behavior of dicarbollide salts, first comparing pure aqueous with nonaqueous (chloroform) solvents, and then focusing on the "oil"/water interface. The most important finding concerns *the surfactant-type behavior of the dicarbollide anions*, which, although lacking the classical amphiphilic topology, tend to self-assemble in aqueous solution as well as at the aqueous interface. The interfacial activity of a given anion is modulated by the nature of its M^{n+} counterions and by the X substituents in the XCD^- series. A remarkable result is the *attraction of hard cations such as* UO_2^{2+} *or* Eu^{3+} *at the interface*, which we believe is a crucial feature as far as the synergistic effect of dicarbollides in ion extraction is concerned. However, before discussing these issues, it is important to ensure that the surface activity of dicarbollides does not result from computational artifacts.

A first issue in molecular dynamics concerns the sampling of the relevant configurations, which must be sufficient to avoid being trapped in metastable states. The most critical case concerns the CCD^- Eu^{3+} salt, whose Eu^{3+} ions concentrate near the interface instead of the bulk water region. As shown above, however, similar distributions were observed when the Eu^{3+} were initially in bulk water or shared between the two liquid phases, indicating that the sampling was sufficient. Further tests are reported below.

Testing Other Water Models. Another issue concerns the representation of solvents whose parameters have been fitted on the bulk liquid properties with a given protocol. Generally, the calculated structure and dynamics of a liquid depend on long-range interaction truncation and temperature control methods,[47] and interfacial and transport properties of TIP3P water obtained with the Ewald summation calculations are further from experiment than the cutoff-based results.[48] The TIP3P water model overestimates the water polarity at the neat interface,[33,49] thereby possibly exaggerating the concentration of ions in that region. The diffusion constant of TIP3P water is also known to be too high compared to experiment.[31,32] This is why we decided to test the more satisfactory TIP5P model[31,32] for the CCD^- Cs^+ and CCD^- Eu^{3+} containing solutions, simulated in the same conditions as above. Furthermore, we investigated the effect of water polarization using the 4P−Pol model[33] in the case of the "hardest" ions, i.e., with the Eu^{3+} salt that accumulated at the interface. With these three water models, the CCD^- anions retain their surface activity, and the majority of cations concentrate at the interface (Figure S5, Supporting Information). There are, however, some differences, which are addressed below.

There are more CCD^- and Cs^+ ions in water and, thus, less at the interface with the TIP5P water (72 and 54%, respectively) than with the TIP3P water (93 and 71%). The same trend is observed with the CCD^- Eu^{3+} ions (70 and 62%, respectively, at the interface with the TIP5P water vs 74 and 68% with the TIP3P water). It thus looks as if the ions are somewhat more hydrophilic and less surface active with the TIP5P than with the TIP3P water.

The dynamics of ions at the interface also depends on the water model. The dicarbollides are less mobile with TIP5P than with TIP3P water, as seen from the diffusion coefficients *D*, following the same trends as neat water itself (see Table S3, Supporting Information). It might thus be feared that the systems are less well equilibrated with TIP5P than with TIP3P water after 2.5 ns. This is not the case, however, as seen upon prolongation of the dynamics with TIP5P water from 2.5 to 5 ns. For both CCD^- Cs^+ and CCD^- Eu^{3+} solutions, the final proportion of anions and cations at the interface (74 and 53%, 63 and 58%, respectively) is quasi the same as after 2.5 ns. The small differences between the TIP3P and TIP5P results stem from the water potential and not from insufficient sampling.

Regarding the effect of water polarizability, one finds even more CCD^- and Eu^{3+} ions at the interface with the 4P−Pol model (85 and 79%, respectively; see Figure S5, Supporting

Information) than with the TIP3P or TIP5P models. This is consistent with the enhanced surface activity of ions when polarization effects are taken into account.[50−52] The major difference with the previous simulations is that the ions diluted onto the two interfaces, i.e., migrated through the water slab from one interface to the other during the dynamics, thereby confirming their interfacial activity.

The extent of cation hydration depends on the water model. Cs^+ is somewhat more hydrated (6.4 versus 5.8 H_2O) and less coordinated to Cl_{CCD} atoms (1.3 versus 2.4 Cl) with the TIP5P than with the TIP3P model, presumably because there are less Cs^+ ions at the interface with the TIP5P model. Regarding Eu^{3+}, it is hydrated by 9.0 H_2O with the TIP3P model, by 9.2 H_2O with the TIP5P model, and by 8.0 H_2O with 4P−Pol model and thus always interacts with CCD^- in its hydrated form.

Effect of the Polarity of the "Oil" Phase. As the OPLS model of chloroform (also noted CHLOR-1) seems not polar enough to properly solvate ions, we simulated the 30 CCD^- Cs^+ ions at the interface using the CHLOR-2 and CHLOR-3 "oil" models, simply obtained by scaling the CHLOR-1 charges by a factor 2.0 or 3.0, respectively (Figure S6, Supporting Information). As expected, increasing the polarity of the oil molecules enhances the intersolvent mixing. The water-in-oil molar fraction increases from 0.0 to 0.015 and 0.395, respectively, while the oil-in-water molar fraction increases from 0.0 to 0.002 and 0.020, respectively from the CHLOR-1, CHLOR-2, and CHLOR-3 models. Even with the most polar model, however, the aqueous and oil phases are separated, forming an interface, and in no case are the Cs^+ CCD^- ions solubilized in the oil phase. All ions remain on the water side of the interface, forming a "diluted layer" that also contains oil molecules. Upon increase of the oil polarity from CHLOR-1 to CHLOR-2, the proportion of ions at the interfaces slightly increases (from 93 to 96% for CCD^-, and from 71 to 73% for Cs^+, respectively), and all ions remain at a single interface. The CHLOR-3 model is too polar and exaggerates the water/chloroform mixing. As a result, there are less CCD^- Cs^+ ions at the interfaces (60 and 67%, respectively) than with the less polar models. When the oil polarity is increased, Cs^+ is more hydrated (5.8 to 6.2 and 6.6 H_2O, on the average, for the CHLOR-1, CHLOR-2, and CHLOR-3 models, respectively).

Effect of Anion Polarizability. In our study, the dicarbollide anions were represented with pairwise additive potentials, and it should be noted that explicitly accounting for their polarizability should further enhance their surface activity, as reported with halide anions,[50−52] thereby strengthening our conclusions on the surfactant behavior of dicarbollides.

On the Surfactant Behavior of Dicarbollide Anions. The Effect of Anion Substituents and Counterions. The simulated surfactant behavior of dicarbollide anions is first supported by experimental data in aqueous solution. After our simulations were completed, there appeared a report on light scattering and microscopic studies of concentrated NaHCD and CsHCD solutions.[44] The authors said that they observed a "completely novel phenomenon, association" of these anions in aqueous solutions. About 80% of NaHCD formed large aggregates (of up to 115 nm) and a small fraction of molecules dissolved molecularly or formed small aggregates. The behavior of nanoaggregates was found to be fairly complex and to depend on the concentration and aging of the solutions and on the counterions. Our microscopic results cannot be directly compared to these data obtained in different conditions and at a mesoscopic scale (ca. 10^{-3} M solutions containing aggregates of ca. 10^5−10^6 anions). However, both approaches are consistent with each other, showing the formation of anionic clusters stabilized by counterions by different extents if one compares Cs^+ to H_3O^+. The simulated aggregates are dynamic in nature, and their size, on the order of 2 nm, also fluctuates with time, involving some anion exchanges between the "cluster" and "bulk water" domains.

Recent surface tension measurements at the water/DCE binary system (DCE = 1,2-dichloroethane) confirm the surface activity of dicarbollide anions.[43] The studies were conducted with CsHCD and NaHCD salts in DCE (typical concentrations ranging from 10^{-7} to 10^{-3} M) in equilibrium with 0.1 M aqueous solutions of metallic salts (generally chlorides). On the basis of their effects on the surface activity, the salts arranged in the order: $Mg^{2+} \approx Ba^{2+} \approx Pb^{2+} > Li^+ \approx Na^+ > K^+ > NH_4^+ > Rb^+ > Cs^+$. Thus, bivalent cations influence more strongly the surface activity of the HCD^- anions than monovalent cations do. It looks as if the HCD^- anions are most attracted from the DCE phase to the interface by the hardest cations that sit in water and vice versa. On the other hand, among the monovalent cations, the more soluble their salt in the organic phase, the poorer is their surface activity. Our simulation results, which correspond to different conditions (dissolution of single dicarbollide salts at higher concentrations), are consistent with the surface activity of these "peanut-shaped" anions and the importance of counterions. They also allow us to compare different XCD^- anions for a given counterion. In the experimental studies,[43] it was speculated that, at the interface, the HCD^- anions form a layer constituted by "a set of rigidly packed cylinders" with a symmetry axis located parallel to the interface, corresponding to a limiting area of 95 ± 8 Å^2 per anion. Such a schematic view is not supported by our simulations, however. Even in the case of the Cs^+ CCD^- or Cs^+ $BrCD^-$ salts for which the proportion of ions at the interface is found to be the highest, the anions are "diluted" at the interface without forming a regular monolayer, as seen, e.g., in the corresponding *xy* planes (Figure 9). In fact, the interfacial surface is rough, and the anions spread about 10 Å away from the average plane of the interface, adopting multiple orientations. In the case of salts with more hydrophilic anions (e.g., HCD^-) or more hydrophilic counterions (Na^+, UO_2^{2+}, Eu^{3+}), the interface is still less covered. In the series of XCD^- Cs^+ salts, and considering only the anions that sit within 10 Å from the interface, one finds an average *xy* area of 163, 135, 95, and 85 Å^2 per anion, respectively, when X = H, Me, Cl and Br, thus decreasing when the interface is more covered. In the CCD^- series with Na^+, UO_2^{2+}, and Eu^{3+} counterions, the interface is less covered, leading to 138, 105, and 113 Å^2, respectively, per anion.

Concerning the effect of M^{n+} counterions at the interface, our results are consistent with well-known trends observed in the stabilization of anionic micelles by counterion condensation.[53,54] Condensation of monovalent ions increases as the latter become softer and less hydrophilic. For instance, in the case of dodecyl sulfate "DS" anions associated with M^+ alkali cations, the critical micellar concentration "cmc" follows the sequence $Cs^+ < K^+ < Na^+ < Li^+$, thus increasing with the hydrophilic character of M^+.[55] The same trend is observed with DS micelles and ammonium counterions: $NBu_4^+ < NPr_4^+ < NEt_4^+ < NMe_4^+$.[56] Conversely, the degree of counterion binding to cationic micelles increases in the order: $Cl^- < Br^-$ < nitrate$^-$ < salicylate$^-$, following the Hofmeister sequence.[57,58] Concerning the effect of counterion charge, multicharged counterions such as Al^{3+} and Ca^{2+} are known to be much more effective promoters of micelle growth than monocharged cations such

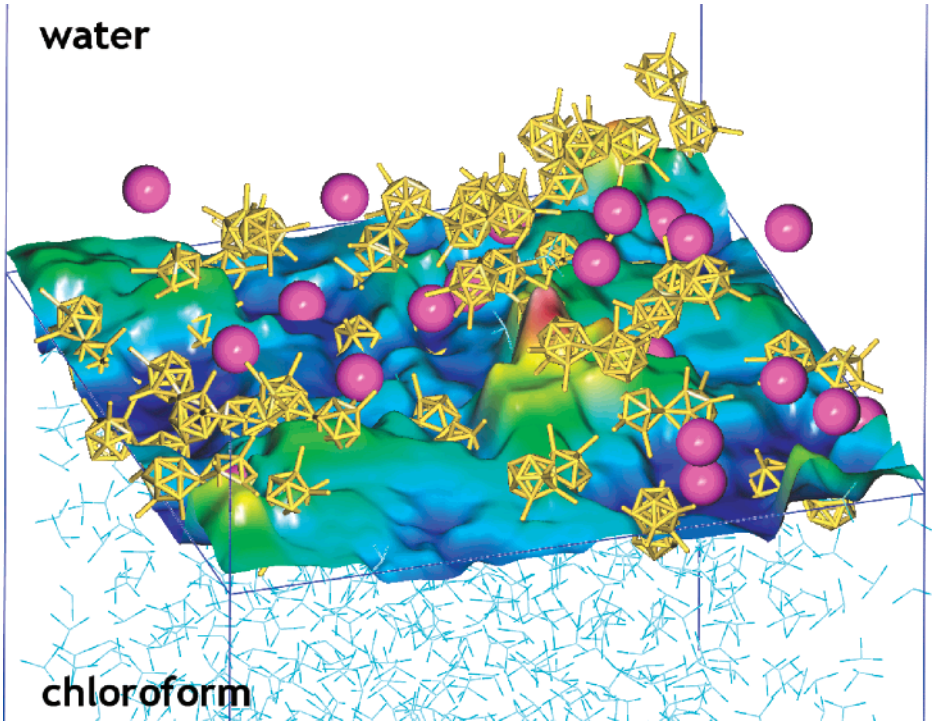

Figure 9. Distribution of all CCD^- anions and of Cs^+ ions within 10 Å from the interface. The surface of the interface is color coded as a function of its *z*-position.

as alkali.[59] This is consistent with the calculated high surface activity or Eu^{3+} and UO_2^{2+} salts of dicarbollides.

There are clear analogies between water/oil and water/air interfaces, onto which soft ions are known to be "attracted".[51] Although lacking the amphiphilic topology, dicarbollide anions are hydrophobic and tend to be expelled out of water in order to avoid paying for a high cavitation energy.[60] On the other hand, at the interface, they still enjoy significant attractive interactions with the water phase as well as with their hydrated counterions. Migration to the oil phase requires electroneutrality and more lipophilic counterions, such as cation complexes with extractant molecules in liquid−liquid extraction.

Interestingly, dicarbollide anions have been recently shown to act as efficient and specific inhibitors of enzymes such as HIV protease.[61] According to X-ray structures,[61] there are two anions "concentrated" in the hydrophobic cleft, surrounded by neutral apolar residues of the enzyme, which is not without analogy with the adsorption of the anions at water/oil interfaces.

On the Synergistic Effect of Dicarbollide Salts on Assisted Ion Extraction. Dicarbollide salts such as $CCD^- Cs^+$ markedly enhance the extraction of metal complexes, likely via a mechanism exchanging their cation (Cs^+, initially in the oil phase) with the hydrophobic ML^{n+} complex formed by M^{n+} and neutral ligands L:

$$n(Cs^+\ CCD^-)_{oil} + mL_{oil} + M^{n+}{}_{wat} \rightarrow nCs^+{}_{wat} + ML_m{}^{n+}{}_{oil} + nCCD^-{}_{oil}$$

As both uncomplexed extractants L and their ML^{n+} complexes are surface active,[62−65] the complexation process is very likely to also occur at the interface provided that the M^{n+} ions concentration is high enough in that very peculiar domain. Generally, hard cations are, however, "repelled" by the interface (as inferred from surface tension measurements,[66] or seen, e.g., from simulations on K^+ Cl^- [67] or Eu^{3+} Cl^- [68] salts at aqueous interfaces; see Figure S7, Supporting Information), preventing their complexation at the interface. In the presence of anionic surfactants such as the simulated dicarbollides, hard cations are attracted at the negatively charged interface, thereby promoting their complexation at the interface. We suggest that this is an important feature of the synergistic effect of dicarbollides in ion extraction. Moreover, surfactants enhance the oil/water mixing, thereby increasing the interfacial area. As seen in bulk water, dicarbollides can form anionic aggregates, ranging from micro- to nanoaggregates, whose surface bears marked analogies with the simulated "planar" interface. Conversely, we find that in an oil-rich mixture, the anions also aggregate of the surface of a micelle, again pointing to the importance of interfacial phenomena in biphasic systems. This is important in liquid−liquid extraction, but also in other processes such as phase transfer catalysis.[69] Further insights will be obtained by considering organic liquids (e.g., alcohols, aromatic solvents) in which dicarbollides are more soluble than in halogenated solvents.

Acknowledgment. We are grateful to IDRIS, CINES, Université Louis Pasteur, and PARIS for computer resources, and Etienne Engler for assistance. We thank University Louis Pasteur for a Ph.D. grant (for G.C.) and EUROPART for support. G.W. thanks Dr. B. Grüner for stimulating discussions.

Note Added after ASAP Publication. This article was published ASAP on April 22, 2006 with a typographical error in ref 7. The revised version was reposted on May 2, 2006.

Supporting Information Available: Figures showing: electrostatic potentials of CCD^- and XCD^- anions; first solvation shell of XCD^- anions; XCD^- H_3O^+ and CCD^- Cs^+ salts in chloroform; cation solvation in the XCD^- Cs^+ and CCD^- M^{n+} solutions at the interface; CCD^- Cs^+ and CCD^- Eu^{3+} salts at the interface; CCD^- Cs^+ salt at the interface simulated with CHLOR-1 to CHLOR-3 chloroform models; hard ions "repelled" by the interface. Tables showing: atomic charges of XCD^- anions obtained by different methods; simulation of 30 XCD^- and 30/n M^{n+} salts; self-diffusion coefficient D calculated

over the last ns. This material is available free of charge via the Internet at http://pubs.acs.org.

References and Notes

(1) Hawthorne, M. F.; Young, D. C.; Wegner, P. A. *J. Am. Chem. Soc.* **1965**, *87*, 1818−1819.

(2) Hawthorne, M. F.; Varadarajan, A.; Knobler, C. B.; Chakrabarti, S. *J. Am. Chem. Soc.* **1990**, *112*, 5365−5366.

(3) Paxton, R. J.; Beatty, B. G.; Hawthorne, M. F.; Varadarajan, A.; Williams, L. E.; Curtis, F. L.; Knobler, C. B.; Beatty, J. D.; Shively, J. E. *Proc. Natl. Acad. Sci. U.S.A.* **1991**, *88*, 3387−3391.

(4) Plesek, J. *Chem. Rev.* **1992**, *92*, 269−278.

(5) Hawthorne, M. F. *Pure Appl. Chem.* **1972**, *29*, 547.

(6) Rais, J.; Selucky, P. *Nucleon* **1992**, *1*, 17.

(7) Rais, J.; Tachimori, S. *Sep. Sci. Technol.* **1994**, *29*, 1347−1365.

(8) Reilly, S. D.; Mason, C. F. V.; Smith, P. H. Report UC-701; LA-11695; Los Alamos National Laboratory: Los Alamos, NM, 1990.

(9) Rais, J.; Grüner, B. In *Ion Exchange and Solvent Extraction*; Marcus, Y., SenGupta, A. K., Marinsky, J. A., Eds.; Marcel Dekker: New York, 2004; Vol. 17, pp 243−324.

(10) Romanovski, V. N.; Smirnov, I. V.; Babain, V. A.; Todd, T. A.; Herbst, R. S.; Law, J. D.; Brewer, K. N. *Solvent Extr. Ion Exch.* **2001**, *19*, 1−21.

(11) Herbst, R. S.; Law, J. D.; Todd, T. A.; Romanovski, V. N.; Babain, V. A.; Esimantovskiy, V. M.; Smirnov, I. V.; Zaitsev, B. N. *Solvent Extr. Ion Exch.* **2002**, *20*, 429−445.

(12) Kyrs, M.; Svoboda, K.; Lhotak, P.; Alexova, J. *J. Radioanal. Nucl. Chem.* **2003**, *258*, 497−509.

(13) Kyrs, M.; Svoboda, K.; Lhotak, P.; Alexova, J. *J. Radioanal. Nucl. Chem.* **2002**, *254*, 455−464.

(14) Smirnov, I. V.; Babain, V. A.; Shadrin, A. Y.; Efremova, T. I.; Bondarenko, N. A.; Herbst, R. S.; Peterman, D. R.; Todd, T. A. *Solvent Extr. Ion Exch.* **2005**, *23*, 1−21.

(15) Alyapyshev, M. Y.; Babain, V. A.; Smirnov, I. V. *Radiochemistry* **2004**, *46*, 270−271.

(16) Reinoso-Garcia, M. M.; Verboom, W.; Reinhoudt, D. N.; Brisach, F.; Arnaud-Neu, F.; Liger, K. *Solvent Extr. Ion Exch.* **2005**, *23*, 425−437.

(17) Grüner, B.; Plesek, J.; Baca, J.; Dozol, J. F.; Lamare, V.; Cisarova, I.; Belohradsky, M.; Caslavsky, J. *New J. Chem.* **2002**, *26*, 867−875.

(18) Grüner, B.; Plesek, J.; Baca, J.; Cisarova, I.; Dozol, J. F.; Rouquette, H.; Vinas, C.; Selucky, P.; Rais, J. *New J. Chem.* **2002**, *26*, 1519−1527.

(19) Coupez, B.; Wipff, G. *C. R. Acad. Sci., Ser. IIc: Chim.* **2004**, *7*, 1153−1164.

(20) Stoyanov, E.; Smirnov Khoplin, I.; Varnek, A.; Wipff, G. *Eurad-waste 1999: Radioactive Waste Management Strategies and Issues*; Davies, C., Ed.; European Commission: Brussels, 2000, p 519.

(21) In the literature, the hexachloro derivative is usually abbreviated by CCD^- rather than $ClCD^-$, which would be more consistent with the studied series.

(22) Case, D. A.; Pearlman, D. A.; Cadwell, J. W.; Cheatham, T. E., III; Wang, J.; Ross, W. S.; Simmerling, C. L.; Darden, T. A.; Merz, K. M.; Stanton, R. V.; Cheng, A. L.; Vincent, J. J.; Crowley, M.; Tsui, V.; Gohlke, H.; Radmer, R. J.; Duan, Y.; Pitera, J.; Massova, I.; Seibel, G. L.; Singh, U. C.; Weiner, P. K.; Kollman, P. A. *AMBER 7*; University of California San Francisco: San Francisco, 2002.

(23) Cornell, W. D.; Cieplak, P.; Bayly, C. I.; Gould, I. R.; Merz, K. M.; Ferguson, D. M.; Spellmeyer, D. C.; Fox, T.; Caldwell, J. W.; Kollman, P. A. *J. Am. Chem. Soc.* **1995**, *117*, 5179−5197.

(24) De Boer, D. G.; Zalkin, A.; Templeton, D. H. *Inorg. Chem.* **1968**, *7*, 2288.

(25) Bühl, M.; Hnyk, D.; Machacek, J. *Chem.—Eur. J.* **2005**, *11*, 4109−4120.

(26) Åqvist, J. *J. Phys. Chem.* **1990**, *94*, 8021−8024.

(27) Guilbaud, P.; Wipff, G. *THEOCHEM* **1996**, *366*, 55−63.

(28) van Veggel, F. C. J. M.; Reinhoudt, D. N. *Chem.—Eur. J.* **1999**, *5*, 90−95.

(29) Jorgensen, W. L.; Chandrasekhar, J.; Madura, J. D.; Impey, R. W.; Klein, M. L. *J. Phys. Chem.* **1983**, *79*, 926.

(30) Jorgensen, W. L.; Briggs, J. M.; Contreras, M. L. *J. Phys. Chem.* **1990**, *94*, 1683−1686.

(31) Mahoney, M. W.; Jorgensen, W. L. *J. Chem. Phys.* **2000**, *112*, 8910−8922.

(32) Mahoney, M. W.; Jorgensen, W. L. *J. Chem. Phys.* **2001**, *114*, 363−366.

(33) Dang, L. X.; Chang, T. *J. Chem. Phys.* **1997**, *106*, 8149−8159.

(34) Frisch, M. J.; Trucks, G. W.; Schlegel, H. B.; Scuseria, G. E.; Robb, M. A.; Cheeseman, J. R.; Montgomery, J. A., Jr.; Vreven, T.; Kudin, K. N.; Burant, J. C.; Millam, J. M.; Iyengar, S. S.; Tomasi, J.; Barone, V.; Mennucci, B.; Cossi, M.; Scalmani, G.; Rega, N.; Petersson, G. A.; Nakatsuji, H.; Hada, M.; Ehara, M.; Toyota, K.; Fukuda, R.; Hasegawa, J.; Ishida, M.; Nakajima, T.; Honda, Y.; Kitao, O.; Nakai, H.; Klene, M.; Li, X.; Knox, J. E.; Hratchian, H. P.; Cross, J. B.; Bakken, V.; Adamo, C.; Jaramillo, J.; Gomperts, R.; Stratmann, R. E.; Yazyev, O.; Austin, A. J.; Cammi, R.; Pomelli, C.; Ochterski, J. W.; Ayala, P. Y.; Morokuma, K.; Voth, G. A.; Salvador, P.; Dannenberg, J. J.; Zakrzewski, V. G.; Dapprich, S.; Daniels, A. D.; Strain, M. C.; Farkas, O.; Malick, D. K.; Rabuck, A. D.; Raghavachari, K.; Foresman, J. B.; Ortiz, J. V.; Cui, Q.; Baboul, A. G.; Clifford, S.; Cioslowski, J.; Stefanov, B. B.; Liu, G.; Liashenko, A.; Piskorz, P.; Komaromi, I.; Martin, R. L.; Fox, D. J.; Keith, T.; Al-Laham, M. A.; Peng, C. Y.; Nanayakkara, A.; Challacombe, M.; Gill, P. M. W.; Johnson, B.; Chen, W.; Wong, M. W.; Gonzalez, C.; Pople, J. A. *Gaussian 03*, revision C.02; Gaussian, Inc.: Wallingford, CT, 2004.

(35) Muzet, N.; Engler, E.; Wipff, G. *J. Phys. Chem. B* **1998**, *102*, 10772−10788.

(36) Berendsen, H. J. C.; Postma, J. P. M.; van Gunsteren, W. F.; Di Nola, A. *J. Chem. Phys.* **1984**, *81*, 3684.

(37) Engler, E.; Wipff, G. *Crystallography of Supramolecular Compounds*; Tsoucaris, G., Ed.; Kluwer: Dordrecht, The Netherlands, 1996, p 471.

(38) Humphrey, W.; Dalke, A.; Schulten, K. *J. Mol. Graphics* **1996**, *14*, 33−38.

(39) Wipff, G.; Engler, E.; Guilbaud, P.; Lauterbach, M.; Troxler, L.; Varnek, A. *New J. Chem.* **1996**, *20*, 403.

(40) Kollman, P. *Chem. Rev.* **1993**, *93*, 2395−2417.

(41) Jorgensen, W. L.; Tirado-Rives, J. *J. Phys. Chem.* **1996**, *100*, 14508−14513.

(42) According to AMBER calculations on the $CCD^-\cdots HOH$ dimer, the interaction energy amounts to −5.2 kcal/mol, in good agreement with the corresponding HF/6-31G* result (−5.1 kcal/mol, with BSSE correction). Furthermore, upon a 1 ns MD simulation on the $HCD^-\cdots HOH$ dimer at 100 K, the H_2O molecule is found to "roll" onto the anion, without finding a well-defined potential well, and corresponds to an average HCD^-/H_2O interaction energy of −4.6 kcal/mol, also in agreement with the HF/6-31G* result (−4.7 kca/mol).

(43) Popov, A.; Borisova, T. *J. Colloid Interface Sci.* **2001**, *236*, 20−27.

(44) Matejicek, P.; Cigler, P.; Prochazka, K.; Kral, V. *Langmuir* **2006**, *22*, 575−589.

(45) Note that, for the CCD^- salt, the distributions of ions obtained with the 6-31G* or 3-21G* charges are similar.

(46) Dupont, J. *J. Braz. Chem. Soc.* **2004**, *15*, 341−350.

(47) Mark, P.; Nillsson, L. *J. Comput. Chem.* **2002**, *23*, 1211−1219.

(48) Feller, S. E.; Pastor, R. W.; Rojnuckarin, A.; Bogusz, S.; Brooks, B. R. *J. Phys. Chem.* **1996**, *100*, 17011−17020.

(49) Archontis, G.; Leontidis, E.; Andreou, G. *J. Phys. Chem. B* **2005**, *109*, 17957−17966.

(50) Chang, T. M.; Dang, L. X. *Chem. Rev.* **2006**, *106*, 1305−1322.

(51) Vrbka, L.; Mucha, M.; Minofar, B.; Jungwirth, P.; Brown, E. C.; Tobias, D. J. *Curr. Opin. Colloid Interface Sci.* **2004**, *9*, 67−73.

(52) Jungwirth, P.; Tobias, D. J. *J. Phys. Chem. B* **2002**, *106*, 6361−6373.

(53) Srinivasan, V.; Blankschtein, D. *Langmuir* **2003**, *19*, 9932−9945 and references therein.

(54) Srinivasan, V.; Blankschtein, D. *Langmuir* **2003**, *19*, 9946−9961.

(55) Rosen, M. J. *Surfactants and Interfacial Phenomena*, 2nd ed.; John Wiley & Sons: New York, 1989.

(56) Bales, B. L.; Tiguida, K.; Zana, R. *J. Phys. Chem. B* **2004**, *108*, 14948−14955.

(57) Cacace, M. G.; Landau, E. M.; Ramsden, J. J. *Q. Rev. Biophys.* **1997**, *30*, 241−277.

(58) Kunz, W.; Nostro, P. L.; Ninham, B. W. *Curr. Opin. Colloid Interface Sci.* **2004**, *9*, 1−18.

(59) Srinivasan, V.; Blankschtein, D. *Langmuir* **2003**, *19*, 9946−9961 and references therein.

(60) Pierotti, R. A. *Chem. Rev.* **1976**, *76*, 717−726.

(61) Cigler, P.; Kozisek, M.; Rezacova, P.; Brynda, J.; Otwinowski, Z.; Pokorna, J.; Plesek, J.; Grüner, B.; Dolckova-Maresova, L.; Masa, M.; Sedlacek, J.; Bodem, J.; Kräusslich, H.-G.; Kral, V.; Konvalinka, J. *Proc. Natl. Acad. Sci. U.S.A.* **2005**, *102*, 15394−15399.

(62) Watarai, H. *Trends Anal. Chem.* **1993**, *12*, 313−318.

(63) Szymanowski, J. *Solvent Extr. Ion Exch.* **2000**, *18*, 729−751.

(64) Coupez, B.; Boehme, C.; Wipff, G. *J. Phys. Chem. B* **2003**, *107*, 9484−9490.

(65) Schurhammer, R.; Berny, F.; Wipff, G. *Phys. Chem. Chem. Phys.* **2001**, *3*, 647−656.

(66) Randles, J. E. B. *Phys. Chem. Liq.* **1977**, *7*, 107−179.

(67) Berny, F.; Schurhammer, R.; Wipff, G. *Inorg. Chim. Acta* **2000**, *300*, 384−394.

(68) Schurhammer, R.; Wipff, G. unpublished.

(69) Sieffert, N.; Wipff, G. *J. Phys. Chem. B* **2006**, *110*, 4125−4134.